Chapter 4

Electrotonic Structure

INTRODUCTION

Chapter 2 introduced the concept of the electrotonic length, L, of a neuron. However, it pointed out that a limitation of cable theory is that it can only be applied to neurons under fairly restrictive conditions. Chapter 3, thus, introduced compartmental models as a completely general framework for studying current flow in neurons. Armed with both cable theory and compartmental modeling, we can now consider how the electrotonic length of real neurons can be estimated and what L means to the computational properties of the neuron.

FINITE CABLE WITH SEALED ENDS, TRANSIENT SOLUTION

All of the solutions to the cable equation that we have considered to this point make the simplifying assumption that the voltage along the cable is varying either as a function of time or a function distance, but not both. This is not realistic because currents flowing in real neurons produce voltages that vary with both space and time. As a last case, we will consider a solution that allows examination of the voltage as a function of both space and time. It is an important case that provides a way to experimentally estimate electrotonic length in real neurons. Charge does not need to be evenly distributed along the length of the cable at an initial time $T = 0$. Figure

4–1A, for example, shows a cable with a finite length. If we assume that there is an initial exponential distribution of charge along the length of the cable, Figure 4-1B shows the voltage that results from the charge distribution at time $T = 0$. The problem is to determine how the voltage subsequently varies as a function of both space and time.

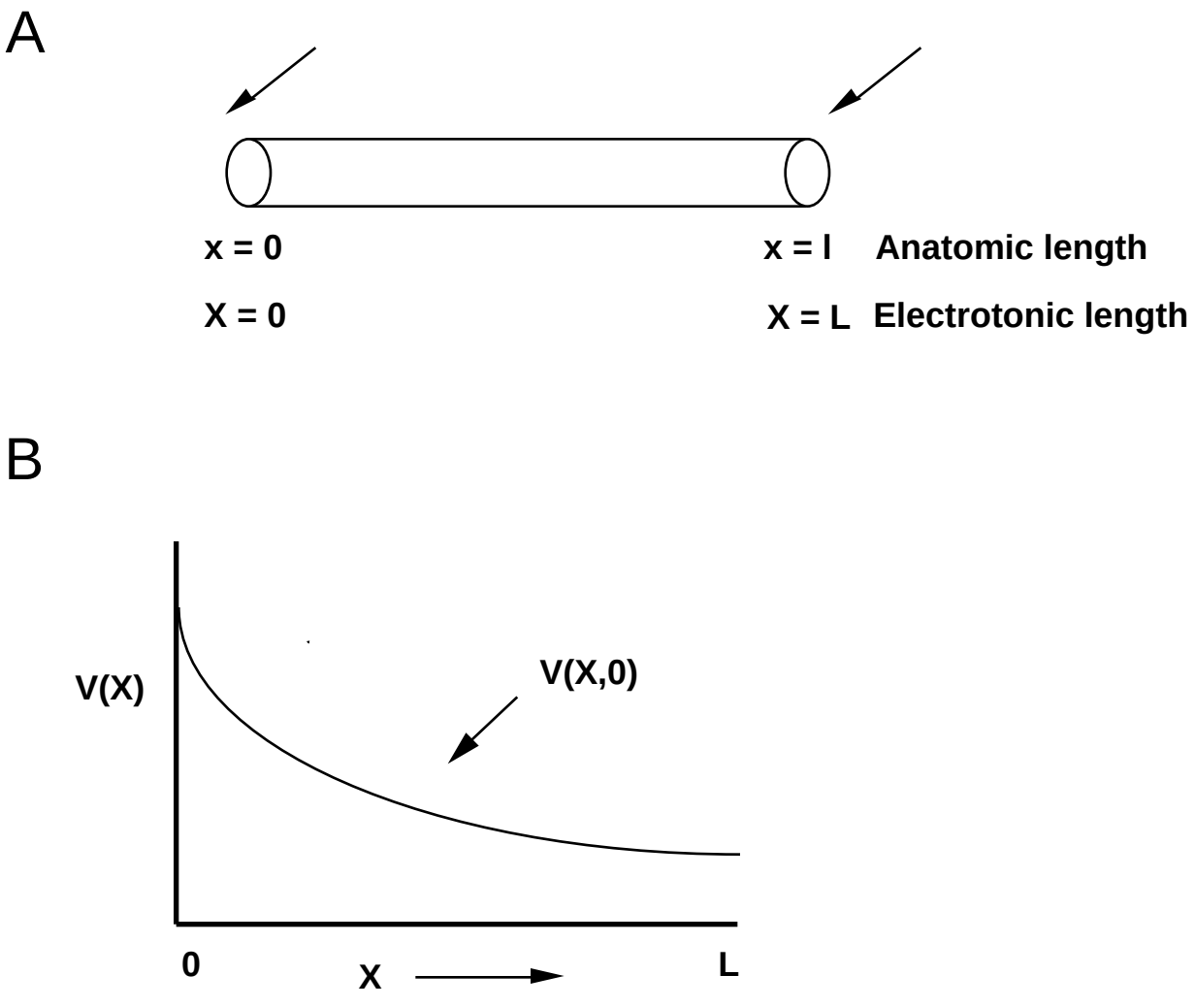

Figure 4-1. Finite cable with sealed ends, transient case. A. finite cable with two sealed ends (arrows). B. Initial distribution of voltage along the length of the cable, plotted as a funciton of electrtonic distance.

In Chapter 2, we considered cases in which voltage was a function of space or time, but not both. However, we now need to consider solutions of the cable equation for which the spatial and temporal factors of $V(X,T)$ are not independent of each other. A useful approach is to introduce a *separation variable ,* α*,* that links the spatial and temporal factors of the solution together. Like a and b in the general solution, it is undetermined and will have to be found from the boundary conditions. Thus, we begin looking for a solution of the cagle equationof the form

(4-1) $$V(\alpha, X, T) = u(\alpha, X)v(\alpha, T) \quad .$$

Our analysis of the space-clamped, infinite cable showed that the charge initially distributed along the cable decayed exponentially with time. The rate of decay was determined by the membrane time constant. It is reasonable to guess, then, that an uneven charge will also decay exponentially and try working with a solution with an exponential time dependence:

(4-2) $$V(\alpha, X, T) = u(\alpha, X)e^{-(1+\alpha^2)T} \quad .$$

Incorporating the separation variable in the exponent as $1+\alpha^2$ appears entirely arbitrary at this point, but will simplify the algebra later in our calculations.

We again use sealed end boundary conditions, but now require that both ends be sealed. The mathematical representation of this is

(4-3) $$\left.\frac{\partial u(\alpha, X)}{\partial X}\right|_{0, L} = 0 \quad .$$

If we substitute the trial solution, Equation (4-2), into the cable equation and evaluate the derivatives, we find that the exponential factor is present in each term of the equation and can be factored out:

(4-4) $$\frac{d^2u(\alpha, X)}{dX^2} + \alpha^2 u(\alpha, X) = 0 \quad .$$

The next steps exactly parallel the calculations for the steady state, semi-infinite cable and lead to a general solution :

$$[D^2 + \alpha^2]u(\alpha, X) = 0$$

(4-5) $$[D + i\alpha][D - i\alpha]u(\alpha, X) = 0 \quad \text{where} \quad i = \sqrt{-1}$$

$$\frac{du(\alpha, X)}{dX} = \pm iu(\alpha, X)$$

$$u(\alpha, X) = ae^{+i\alpha X} + be^{-i\alpha X} \quad .$$

If we use the relationships

(4-6) $$e^{i\alpha x} = \cos\alpha x + i\sin\alpha x \quad \text{and} \quad e^{-i\alpha x} = \cos\alpha x - i\sin\alpha x \,,$$

between exponentials and sines and cosines and do some algebra, we obtain

(4-7) $$u(\alpha, X) = (a + b)\cos\alpha X + i(a - b)\sin\alpha X \quad .$$

We set $a = b$ in order to avoid having an imaginary term and

(4-8) $u(\alpha, X) = 2a\cos\alpha X = B\cos\alpha X$, where $B = 2a$.

Taking the derivative of $u(\alpha, X)$ with respect to X gives

(4-9) $$\frac{du(\alpha, X)}{dX} = -B\sin\alpha X \quad .$$

This derivative vanishes at $X = 0$ and can be made to also vanish at $X = L$ by assigning a value of $\alpha = n\pi / L$, where $n = 0,1,2,3,\ldots$. This works because

(4-10) $$\sin\alpha L = \sin\left[\frac{n\pi}{L}(L)\right] = \sin[n\pi] = 0$$

for all integer values of n. It means that there are an infinite number of solutions, but the sum of all of these solutions is also a solution. Thus, we have

(4-11) $$V(\alpha, X, T) = \sum_{n=0}^{\infty} B_n \cos\left[\frac{n\pi}{L}\right] Xe^{-(1+\alpha_n^2)T} \quad .$$

Notice that we've indexed the coefficients, B_n, with n and also anticipated the possbility that the separation variable, α, is different for each term by indexing it as α_n, as well.

The values of the coefficients, B_n, can be determined using the initial voltage distribution, $V(X,0)$. If we set $T = 0$, then

(4-12) $$V(X,0) = \sum_{n=0}^{\infty} B_n \cos\left(\frac{n\pi}{L}\right)X \quad .$$

The coefficients are determined using special properties of the integrals of cosine functions. Multiply both sides of Equation 4-12 by $\cos\left(\frac{m\pi}{L}\right)X$ and integrate both sides of the equation

(4-13) $$\int_0^L \cos\left(\frac{m\pi}{L}\right)XV(X,0)\,dX = \int_0^L \sum_{n=0}^{\infty} B_n \cos\left(\frac{m\pi}{L}\right)X \cos\left(\frac{n\pi}{L}\right)X\,dX \quad .$$

The special property is that

(4-14) $$\int_0^L \cos\left(\frac{m\pi}{L}\right)X \cos\left(\frac{n\pi}{L}\right)X\,dX = \delta_{m,n}$$

where $\delta_{m,n}$ is called the *Kronecker delta function*. It is equal to 1 when $m = n$ and 0 when $m \neq n$ All of the terms on the right hand side of the equation vanish except the one for which $m = n$, and

(4-15) $$B_n = \int_0^L \cos\left(\frac{n\pi}{L}\right)XV(X,0)\,dX$$

This equation can be simplified by defining a set of new coefficients

(4-16) $$C_n = \cos\left(\frac{n\pi}{L}\right)X \int_0^L \cos\left(\frac{n\pi}{L}\right)XV(X,0)\,dX$$

so that

(4-17) $$V(X,T) = \sum_{n=0}^{\infty} C_n e^{-(1+\alpha_n^2)T} \quad .$$

Remember that $T = t/\tau$ where τ is the membrane time constant. To help make the nomenclature internally consistent, set $\tau = \tau_o$ and define

(4-18) $$\frac{\tau_o}{\tau_n} = 1 + \alpha_n^2 = 1 + \left[\frac{n\pi}{L}\right]^2$$

Thus

(4-19) $$\left[\frac{\tau_o}{\tau_n}\right][T] = \left[\frac{\tau_o}{\tau_n}\right]\left[\frac{t}{\tau_o}\right] = \frac{t}{\tau_n}$$

and

(4-20) $$e^{-(1+\alpha_n^2)T} = e^{-t/\tau_n}$$

for each value of n. There are, thus, a series of time constants, of which τ_o is the largest. The solution to the cable equation is given, finally, by

(4-21) $$V(x,t) = C_o e^{-t/\tau_o} + C_1 e^{-t/\tau_1} + C_2 e^{-t/\tau_2} + \ldots$$

The voltage along the cable is an infinite series of exponential terms. The time constant for the first term is τ_o, which we have set equal to the membrane time constant. The other time constants are called *equalizing time constants*. τ_1 is the first equalizing time constant, τ_2 is the second equalizing time constant, etc.

To understand the significance of the time constants, let's consider the meaning of the coefficients, C_n, in more detail. They correspond to the coefficients of a *Fourier expansion* of the initial voltage distribution. The French mathematician, Fourier, showed that many mathematical functions, $y(x)$, can be expressed as an infinite series of sine and cosine terms

(4-22) $$y(x) = \sum_{n=0}^{\infty} A_n \sin n\pi x + B_n \cos n\pi x \quad .$$

The coefficients in the expansion can be determined in the same way we determined the coefficients in the cable equation, taking advantage of the special properties of the integrals of products of sines and cosines. The boundary conditions in the finite cable problem require that the coefficients of the sine terms be zero. The coefficients of the cosine terms are obtained by integrating the product of the initial voltage distribution and a cosine term. The initial voltage distribution is, thus, being regarded as a sum of many component voltage distributions. The first of these is a uniform distribution that is distributed along the length of the cable. The second is a cosine function with a relatively long wavelength. The third, fourth, etc. distributions are cosine functions with progressively smaller wavelengths. The exponential function in each term of the solution determines the rate at which the particular voltage distribution is decaying to zero. We have already solved this problem in the case of the zero order term in which a uniform voltage distribution decays to zero and this time constant is the membrane time constant. It describes the rate at which the voltage distribution resulting from an evenly distributed charge decays to zero. The

exponential in the second term describes the rate at which a voltage description described by the cosine function $\cos\left[\frac{n\pi x}{L}\right]$ decays to zero, etc. Thus, each successive term describes the rate at which progressively more local voltage distributions become equalized along the cable. This solution to the cable equation provides some insights into current flow in the cable, but it is also the basis of an experimental means of measuring the electrotonic length.

MEASURING ELECTROTONIC LENGTH

The key to experimentally measuring the electrotonic length of a neuron is to recognize that the time constants in Equation (4-21) are all functions of the electrotonic length, L. This is the point of Equation (4-18):

(4-23) $$\frac{\tau_o}{\tau_n} = 1 + \alpha_n^2 = 1 + \left[\frac{n\pi}{L}\right]^2$$

and

(4-24) $$L = \frac{n\pi}{\left[\tau_o / \tau_n - 1\right]^{1/2}}$$

In the case of $n = 1$, the electrotonic length is given by

(4-25) $$L = \frac{\pi}{\left[\tau_o / \tau_1 - 1\right]^{1/2}} \quad .$$

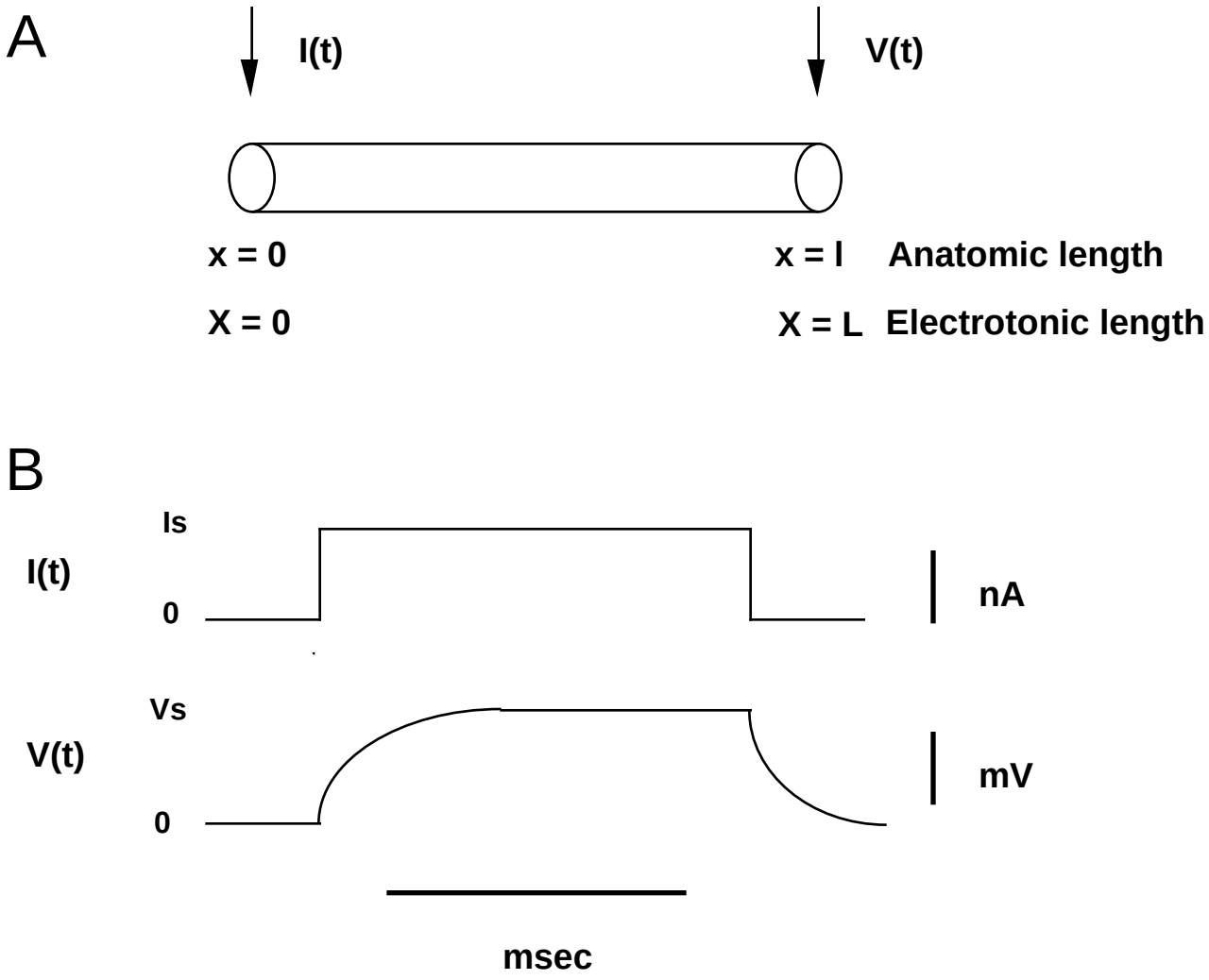

Figure 4-2. Measuring electrotonic length. A. Diagram of the experimental paradigm used to measure electrotonic length. A current is injected at the left end of the cable and the resulting voltage transient measured at the right end. B. Waveforms of the stimulating current (top trace) and the measured voltage transient (bottom trace).

So, we can calculate the electrotonic length of the cable from this simple equation by measuring the membrane and first equalizing time constants.

This is possible using modern intracellular recording electrodes that allow the injection of a current into a cell and the recording of a resulting voltage transient. Figure 4-2 shows the idea of the experiment. A cell is impaled with the electrode and a square current pulse of amplitude, I_s, and

duration of 500 msec is injected into the cell. This produces a voltage transient that increases from the resting membrane potential of the cell to a steady-state value of V_s. The magnitude of V_s is determined by the total input resistance, R_N , of the cell and Ohm's law: $V_S = I_S R_N$. When the cell has reached steady-state, charge has been distributed throughout the cell and we could, in principle, measure the voltage at each point on the cell and determine the initial voltage distribution, $V(X,0)$. A particularly nice feature of Rall's method is that we do not actually have to measure the distribution to estimate the time constants in Equation 4-21. When the current injection is terminated, the charge will leak through the membrane and the membrane potential decays back to its resting value, so $V(x,t) = 0$. We can represent this process, using a variant of Equation 4-21, as

(4-26) $$V(x,t) = V_s[1 - C_o e^{-t/\tau_o} - C_1 e^{-t/\tau_1} - C_2 e^{-t/\tau_2} - ...] \quad .$$

The series expansion we used to solve the boundary value problem contains an infinite number of terms. In practice, however, it is usually possible to measure only the first two time constants. Equation 4-2, thus, simplifies to

(4-27) $$V(x,t) = V_s[1 - C_o e^{-t/\tau_o} - C_1 e^{-t/\tau_1}]$$

or

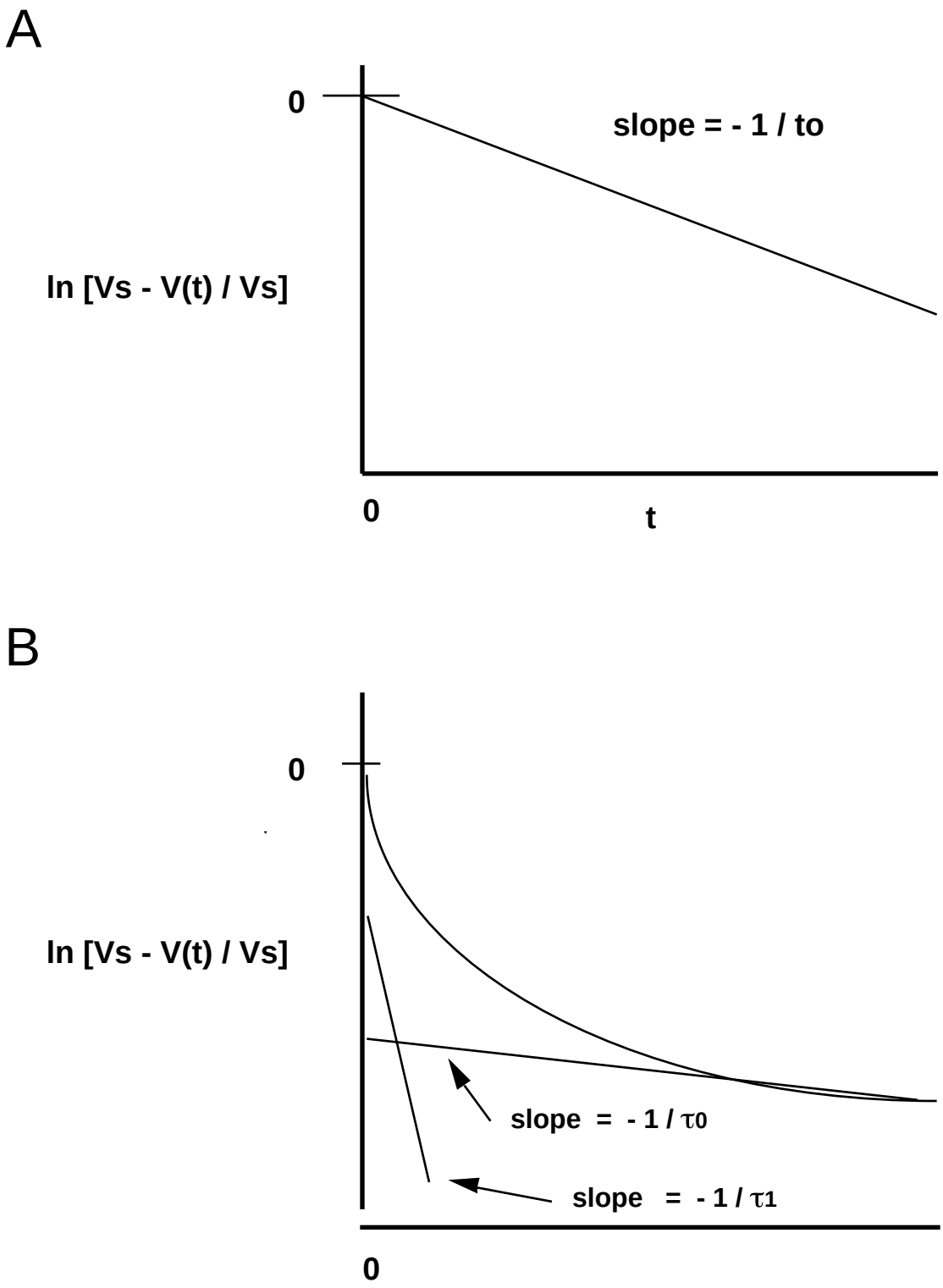

Figure 4-3. Analyzing data from measurements of electrotonic length. A. Voltage transient from an isopotential neuron. A semi-logarithmic plot is linear with the slope equal to the negative reciprocal of the membrane time constant. B. voltage transient from a non-isopotential neuron. The semi-logarithmic plot is non-linear and equals the sum of two straight lines. One represents the membrane time constant; the second results from the first equalizing time constant.

(4-28) $$\frac{V_s - V(x,t)}{V_s} = C_o e^{-t/\tau_o} - C_1 e^{-t/\tau_1}$$

(4-29) $$\ln[\frac{V_s - V(x,t)}{V_s}] = \ln[C_o e^{-t/\tau_o} + C_1 e^{-t/\tau_1}] \quad .$$

It is clear that plotting the left hand side of Equation 4-29 as a function of time in a semi-logarithmic plot will not produce a straight line, as it did in our earlier analysis. The plot is, instead, a curvilinear one like that shown in Figure 4-3B. However, if we use only relatively large time values in constructing the plot, the second term will be close to zero and can be ignored. The resulting semilogarithmic plot will then be linear like the one in Figure 4-3A and can be used to estimate the first time constant, τ_o, and the coefficient, C_o, from the slope and intercept of the plot, respectively. We can then use this linear plot to extrapolate the contributions of the first term to the membrane voltage for short time values. These voltage values are subtracted from the total voltage, and a semilogarithmic plot of the differences as a function of time produces a second linear plot with a greater slope (Fig. 4-3B). This slope is the reciprocal of the second time constant τ_1. The curvilinear plot is, thus, the sum of the two exponential terms. The two time constants are all that is required to calculate the electrotonic length of the neuron. This is the classical way of determining two or more time constants for a process that can be represented as a sum of exponential terms. It is called the method of *peeled exponentials* (Rall, 1969a,b) because each time constant is "peeled" in succession from the semi-logarithmic plot. The value of L estimated in this way is sometimes called L_{peel} (Homes and Rall, 1992b). The process of manually peeling

exponentials is now seldom used because a number of software packages automatically find the values of the time constants and coefficients that best fit the experimental data. However, the time constants obtained this way can also be used to calculate L_{peel} using Equation 4-25.

Measurements of the electrotonic lengths of neurons have been made using the method just outlined. However, they are subject to variety of experimental errors and variations of the basic equations have been developed to compensate for these errors. One factor is that impaling the neuron with a sharp electrode damages the membrane of the cell and permits current to leak out of the cell around the electrode, producing what is known as a *somatic shunt*. Durand (1984) developed an alternative equation for L_{peel} that compensates for the presence of a somatic shunt in estimating the electrotonic length of a neuron. More recently, whole cell patch-clamp methods have been used to estimate electrotonic lengths (Jackson, 1992; Spruston and Johnston, 1992; Staley et al., 1992). The patch clamp method involves establishing a high resistance or *gigohm seal* between the electrode and the cell membrane. This reduces the amount of current that leaks around the electrode and decreases the error produced by shunting of current.

A second difficulty is that the membrane of a real cell typically has voltage-gated conductances that can be activated when current is injected in the cell. Many cells have so-called *inwardly rectifying conductances* (we will discuss these in a later Chapter) that cause the voltage transient to "*sag*" back towards rest from its steady state value. These conductances can

lead to spurious estimates of the electrotonic length. Voltage values from

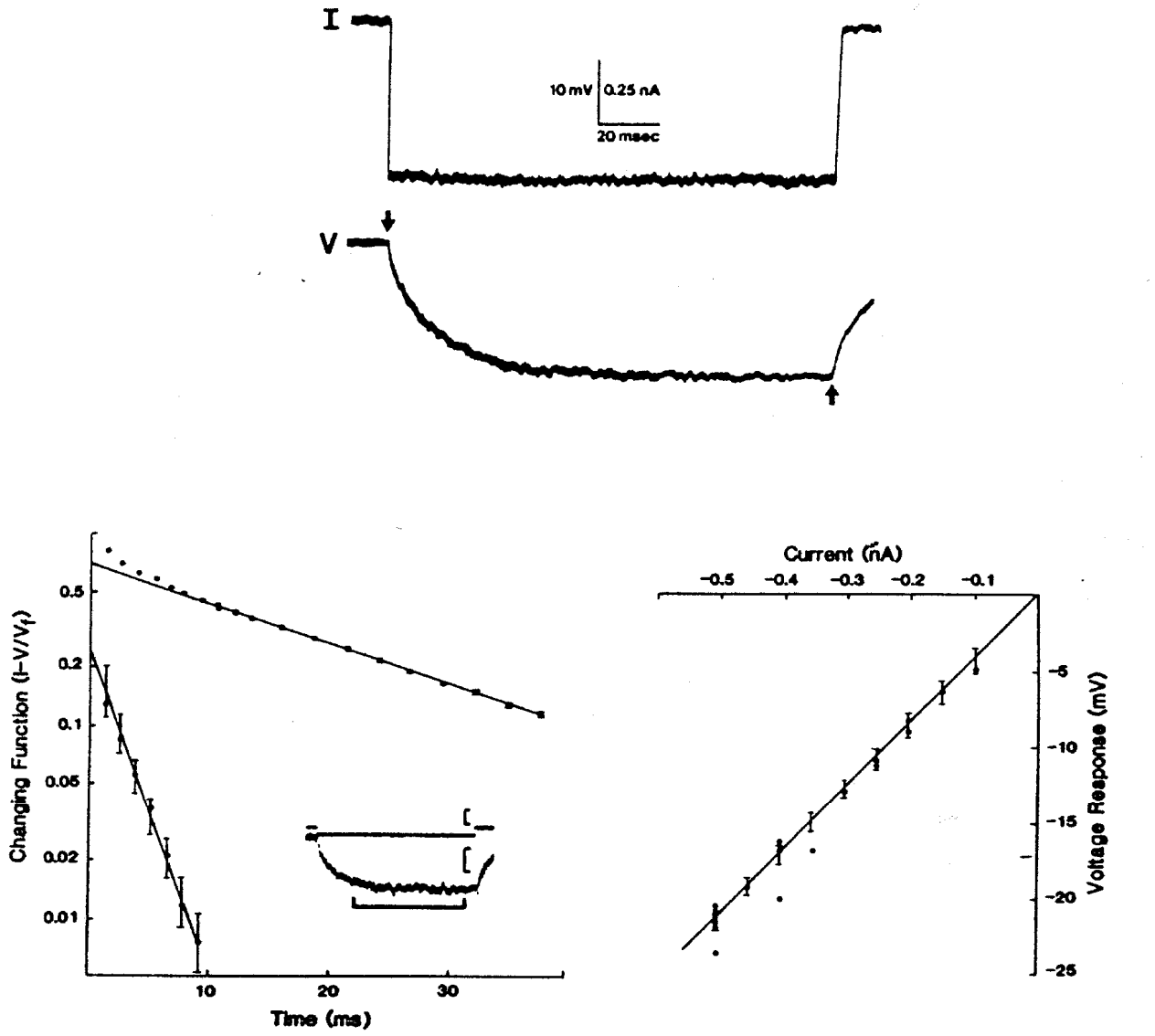

Figure 4-4. Measurement of electrotonic length in a hippocampal pyramidal cell. A. Experimental records of stimulus current (top trace) and resulting voltage transient (bottom trace). B. Semi-logarithmic plot of membrane potential plotted as a charging function. Dots are data points sampled at discrete time intervals. The straight line is a best-fit to voltages measured at longer time points. The slope of this line is related to the membrane time constant. The second line was obtained by extrapolating data points from the estimated membrane time constant and subtracting them from the data point. This line is related to the first equalizing time constant. C. Steady-state voltage response plotted as a function of the injected current. The data are linear, suggesting that the voltage transient is not contaminated by voltage-gated conductances. From Turner (1984).

the decaying phase of the voltage response are, consequently, usually not used to estimate electrotonic lengths because they are often contaminated by activation of voltage-gated channels. Voltage values from the rising phase of the voltage response are less apt to be contaminated, and one method of minimizing contamination of the voltage transient by voltage-gated conductances is to use very short current pulses (Durand et al., 1983; lanasek and Redman, 1973). Other complications are that most neurons are not geometrically well represented as cylinders and do not have membrane properties that are the same all over the neuron. A complete discussion of the modifications needed to correct these factors is beyond the scope of this book. Readers interested in this subject should consult papers by Holmes and Rall (1992a), Kawato (1984), Poznanski (1987, 1991) and Strain and Brockman (1975) for detailed accounts.

FUNCTIONAL IMPLICATIONS OF ELECTROTONIC LENGTH

To understand the functional significance of electrotonic length, we can consider hippocampal pyramidal cells. Figure 4-4 shows the results of one experimental measurement of the electrotonic length of a CA1 pyramidal cell (Turner, 1984). Electrotonic lengths for hippocampal pyramidal cells range between 0.88 and 0.96 (Brown et al., 1981; Johnston, 1983; Turner, 1984; Turner and Schwartzkroin, 1980, 1983; Migliore et al., 1995). This means both types of pyramidal cells introduced early in Chapter 1 are electrotonically compact and current flowing into one part of the neuron will have a noticeable effect on other parts. To get some feeling for what these numbers mean, lets do a rough calculation to see how effective synaptic currents resulting from the mossy fibers on a CA3 pyramidal cell and

Schaffer collaterals on a CA1 pyramidal cell would be. Measurements of the membrane time constants for hippocampal neurons using patch-clamp methods produce higher values than those obtained with sharp electrodes (Spruston and Johnston, 1992). However, using the data for the CA1 pyramid from the experiment shown in Figure 4-4 we would have τ_o = 17.9 msec and τ_1 = 2.04 msec. Our estimate of L_{peel} would then be

(4-30) $$L_{peel} = \frac{\pi}{[17.9/\ 2.04 - 1]^{1/2}} = \frac{3.14}{2.8} = 1.1 \quad .$$

If we think of the proximal shaft of the apical dendrite of the CA1 pyramid as a finite cable that is 300 μm in length, the space constant for the dendrite is 273 μm. If a Schaffer collateral synapse is positioned 200 μm from the soma, it has an electrotonic distance of 200 μm/273 μm = 0.7 from the soma. Suppose the synaptic current produces a voltage of 10 mV at the site of the synapse. Then the resulting voltage at the soma end of the cable will be

(4-31) $$V(X) = \frac{V_o \cosh(L - x)}{\cosh L} = \frac{(10mV)\cosh[1.1 - 0.7]}{\cosh(1.1)} = \frac{(10)(1.1)}{1.7} mV = 6.5mV$$

So, a synaptic potential of 10 mV results in a smaller, but still significant, potential of 6.5 mV at the soma. Comparable data for the CA3 pyramidal cell are τ_o = 21.1 msec, τ_1 = 3.6 msec, and 320 μm. You should do the calculation for a mossy fiber synapse that produces a 10 mV synaptic potential 50 μm from the soma.

Measurements of L_{peel} provide some global concept of how current flows through the neuron, but are very limited in what they can say about the detailed patterns of current flow between the various dendritic branches and the soma. The next section sets the stage for more accurate considerations by beginning a theoretical discussion of the geometric factors involved in current flow in neurons.

SCALING IN NEURONS

Hippocampal pyramidal cells have several features in common, but also show major variations in size and shape. One kind of variation occurs due to embryonic development. The brains of embryos are smaller than those of adults, and -- to some extent -- individual motoneurons or pyramidal cells in embryonic or fetal brains are smaller than the same types of neurons in adult brains. The other kind of variation occurs in different species due to evolutionary changes. The brains of mice are much smaller than those of elephants and hippocampal pyramidal cells in mice are smaller than the same types of neurons in elephants. Since the electrotonic structures of both types of neurons depend in part upon the lengths and diameters of their somata, axons and dendrites, motoneurons and pyramidal cells in mice may have significantly different electrotonic structures than pyramidal cells in elephants.

This is a case in which we can understand the basic problem by relying upon linear cable theory, and thereby avoid the complexities of trying to build full compartmental models of the neurons in questions. The issue is to understand how the electrotonic structure of a neuron changes (or *scales*)

as its dimensions vary, due to either developmental or evolutionary processes. If we think of a neuron as a finite cable with anatomical length l, and a characteristic length, λ, then its electrotonic length is given by

(4-32) $$L = \frac{l}{\lambda} = \frac{2l}{\sqrt{d}} \left[\frac{R_m}{R_a}\right]^{1/2}$$

This means that for particular values of membrane and axial resistance, the electrotonic length varies in direct proportion to the length of the neuron (cable) but inversely with its (diameter)$^{1/2}$.

There are two different ways in which neuronal growth could occur (Hill et al., 1994). The first is *isometric growth* in which the length and diameter of the cable changes at the *same* rate. It is a simple algebra exercise to verify that isometric growth results in larger neurons with larger electrotonic lengths. If a finite cable increases in length by a factor, l_g, and diameter by a factor d_g, then the electrotonic length of the larger cable, L_{large}, is

(4-33) $$L_{large} = \frac{2 l_g l_{small}}{\sqrt{d_g d_{small}}} \left[\frac{R_m}{R_a}\right]^{1/2} = \frac{l_g}{\sqrt{d_g}} L_{small}$$

where L_{small}, l_{small}, and d_{small} are the electrotonic length, anatomic length and diameter, respectively, of the smaller cable. For isometric growth, $l_g = d_g$ and

(4-34) $$L_{large} = \sqrt{l_g} L_{small}$$

That is, the electrotonic length of the cable increases in proportion to the square root of the growth factor, l_g. Isometric growth would lead to a situation in which the Schaffer collaterals synapsing upon CA1 pyramids in elephants are much less effective than those in mice -- everything else being equal.

The second extreme situation is *isoelectrotonic growth*. This would occur if the lengths and diameters of neuronal processes varied at different rates in a way that keeps the electrotonic length of the cable constant, eventhough its dimensions are changing. A little algebra shows this occurs if the cable increases in diameter by a factor $\sqrt{d_g} = l_g$. The electrotonic length of the cable can be preserved only if the neuron exhibits *allometric growth* in which its length and diameter increase at *different* rates. The Schaffer collaterals would have approximately the same effect at the soma in elephants in this case, even though they were anatomically more distant than in mice. These are extreme cases and individual kinds of neurons could exhibit intermediate kinds of growth which involved less increase in electrotonic length than would occur with pure isometric scaling.

Bekkers and Stevens (1990) studied Golgi preparations of neurons in the dentate gyrus and area CA1 in cats and humans to determine whether they show isometric or isoelectronic scaling. They found that both classes of neurons have the same general shape in cats and humans. Human dentate gyrus granule cells had dendrites that were 3.5 times longer than those in cats, but roughly the same diameters. CA1 pyramidal cells had dendrites that were 1.4 times longer in humans than in cats and diameters of about

1.6 µm versus 0.64 µm. These factors were consistent with isoelectrotonic scaling for CA1 pyramids while granule cells clearly do not scale isoelectrotonically. The reason for the scaling differences between the two types of cells is not clear. Bekkers and Stevens suggest that granule cell activity may be less dependent upon the activity of an individual synapse than are CA1 pyramids, so the effective distance of any one synapse from the soma may have little significance in the integrative biology of the granule cells.

Hill *et al.* (1994) were able to draw some functional conclusions by studying two invertebrate neurons that have a clearer relationship to the behavior than do the cells of the hippocampus (Fig. 4-5). One of the neurons they studied was the medial giant interneuron (MGI) of the cricket, *Acheta domesticus*. This neuron is part of an air motion detection system that helps the cricket escape from predators and also plays a role in the recognition of stridulation (that is, chirping) in male crickets. It receives synaptic inputs from sensory neurons that respond to low-frequency air currents. As baby crickets grow, they proceed through a series of instar stages and become progresssively larger. The MGI neurons, however, conserve their frequency and intensity response characteristics during the maturation process. The second neuron Hill et al. studied is the lateral giant interneuron (LG) of the crayfish, *Procambarus clarkii*. This neuron triggers a somersault tailflip after phasic stimulation of the abdomen that allows the animal to escape from predators (Wine, 1984). LG receives mechanosensory inputs through two different pathways. The response properties of the LG neurons change during maturation, consistent with a change in the threshold of the escape response.

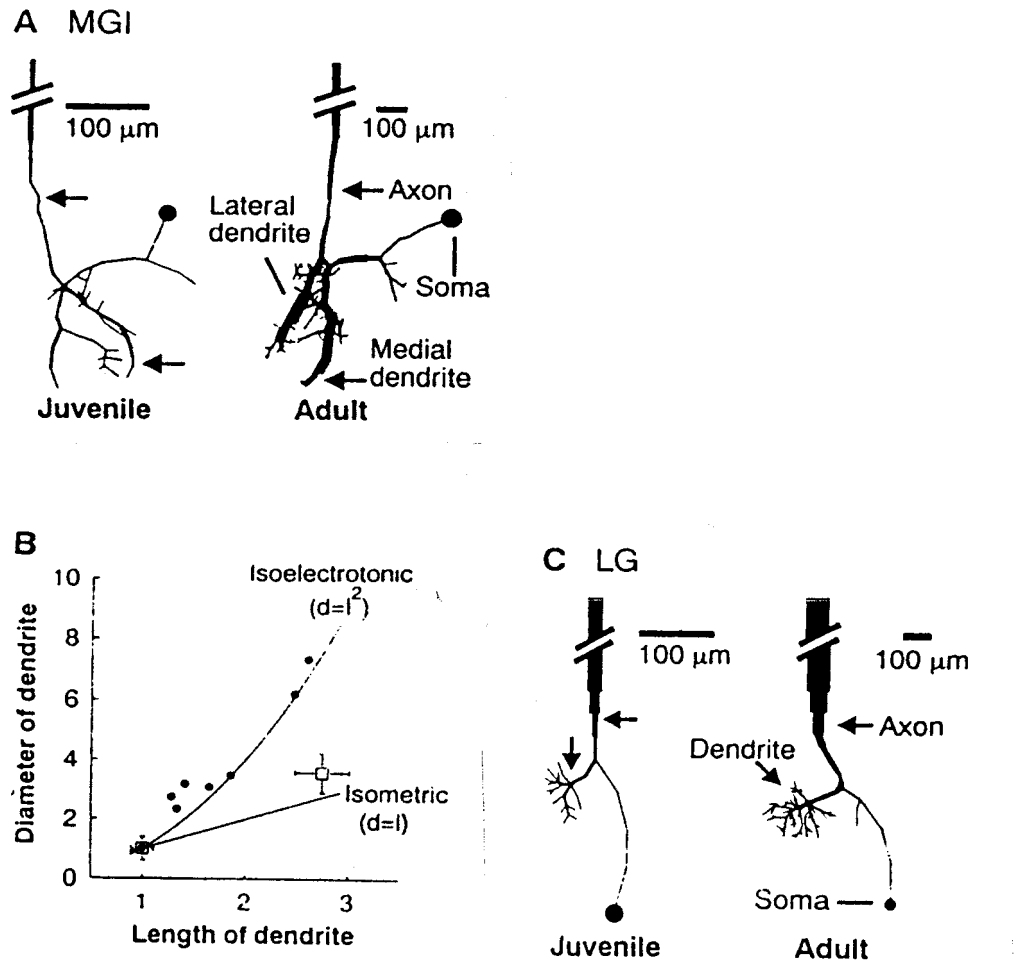

Figure 4-5. Scaling in invertebrate neurons. A. Medial giant interneurons in juvenile and adult crickets. B. Diameter of dendrite plotted as a function of length of dendrite for the medial giant (top) and lateral giant (bottom) interneurons. The medial giant shows isoelectrotonic scaling while the lateral giant shows isometric scaling. C. Lateral giant interneuron in juvenile and adult crayfish. From Hill et al. (1994).

Both types of neurons were studied by impaling them with microelectrodes filled with Lucifer Yellow. Neurons were filled with the marker substances in a series of developmental stages, dehydrated and then cleared so that the dimensions of individual processes could be measured.

The neurons were observed with *confocal microscopy* so estimates of shrinkage (between 52 % and 82 %) could be made. The measurements indicated that neither type of neuron follows the 3/2 power law, and compartmental models were constructed. Figure 4-5B shows a plot of the diameter of the dendrite in both types of neurons as a function of the length of the dendrite for a series of developmental stages. The predicted relationships for isoelectrotonic and isometric growth are shown. The MGI neuron grows in an approximately isoelectronic mode while the LG neuron grows in an approximately isometric mode. Simulations with the compartmental models show that -- as expected -- steady state electrical potentials in MGI neurons showed similar attenuations in small and large neurons while potentials in LG neurons were less effective in large LG neurons than in small ones. However, there is some reason to suspect that these differences do not occur in the real LG neurons. Measurements of the crayfish LG's time constant shows that it increases 2.4 times from 8.6 msec to about 20.9 msec as the animal grows from 1 cm in length to a 10 cm adult animal (Edwards *et al*., 1994a). Simulations with the adult LG cell model show that this 2.4-fold increase in τ_m would reduce the steady-state attenuation from the distal dendrite to the initial axon segment to the level measured in a juvenile LG model. Thus, even though the LG neuron does not show isoelectrotonic growth, it is possible that the efficiency of distal synapses is maintained by developmental changes in the membrane properties of the cell. Everything else is not equal ! This is not an isolated finding in that variations in the membrane time constant have been reported in the development of other neurons such as goldfish retinal ganglion cells (Bloomfield et al, 1991), neurons in a brainstem auditory structure (the

superior olivary nucleus) in rats (Kandler and Fiauf, 1995) and rat neocortical pyramidal cells (McCormick and Prince, 1987).